

Synthesis, Optimization, and Evaluation of Novel Small Molecules as Antagonists of WDR5-MLL Interaction

Yuri Bolshan,^{†,§} Matthäus Getlik,[‡] Ekaterina Kuznetsova,[†] Gregory A. Wasney,[†] Taraneh Hajian,[†] Gennadiy Poda,[‡] Kong T. Nguyen,[†] Hong Wu,[†] Ludmila Dombrowski,[†] Aiping Dong,[†] Guillermo Senisterra,[†] Matthieu Schapira,[†] Cheryl H. Arrowsmith,[†] Peter J. Brown,[†] Rima Al-awar,[‡] Masoud Vedadi,^{*,†} and David Smil^{*,†,§}

[†]Structural Genomics Consortium, University of Toronto, 101 College Street, MaRS Centre, South Tower, Toronto, Ontario M5G 1L7, Canada

[‡]Medicinal Chemistry Platform, Ontario Institute for Cancer Research, 101 College Street, MaRS Centre, South Tower, Toronto, Ontario M5G 0A3, Canada

Supporting Information

ABSTRACT: The WD40-repeat protein WDR5 plays a critical role in maintaining the integrity of MLL complexes and fully activating their methyltransferase function. MLL complexes, the trithorax-like family of SET1 methyltransferases, catalyze trimethylation of lysine 4 on histone 3, and they have been widely implicated in various cancers. Antagonism of WDR5 and MLL subunit interaction by small molecules has recently been presented as a practical way to inhibit activity of the MLL1 complex, and *N*-(2-(4-methylpiperazin-1-yl)-5-substituted-phenyl) benzamides were reported as potent and selective antagonists of such an interaction. Here, we describe the protein crystal structure guided optimization of prototypic compound **2** ($K_{\text{dis}} = 7 \mu\text{M}$), leading to identification of more potent antagonist **47** ($K_{\text{dis}} = 0.3 \mu\text{M}$).

KEYWORDS: WDR5, MLL, SET1 methyltransferase complex, peptide binding site, small molecule antagonists

The SET1-family of human histone methyltransferases (SET1A, SET1B, MLL1, MLL2, MLL3, and MLL4) contribute to active chromatin via mono-, di-, and trimethylation of lysine 4 on histone H3.^{1–3} MLLs are *S*-adenosyl methionine (SAM) dependent lysine methyltransferases that work optimally when in complex with other components; WDR5 (WD40 repeat protein 5), RbBP5 (retinoblastoma-binding protein-5), ASH2L (absent small homeotic disks-2-like), and DPY-30 (WRAD).⁴ WDR5 has been shown to be essential for complex integrity and for fully activating MLL methyltransferase function.^{5–7}

In the peptide-bound structure, WDR5 adopts a donut-shaped WD40-repeat fold with a deep central cavity that normally accommodates an arginine side chain of interacting peptides.⁸ WDR5 binds to the “WDR5 INteracting” (WIN) motif of MLL1 through the peptidyl arginine-binding cleft.^{8–12} A crystal structure of WDR5 in complex with MLL1 WIN peptide revealed the critical role of arginine 3765 of MLL1 in complex formation.⁹ A similar interaction has been reported for WDR5 and the WIN region of all SET1 family lysine methyltransferases, with reported K_{D} values of 1.13, 0.16, 2.03, 0.03, 0.26, and 0.10 μM for MLL1-4, SET1A, and SET1B WIN peptides, respectively.¹³ Although there is significant divergence in the amino acid sequences of WIN motifs close to the critical arginine residue, the plasticity of the WDR5 arginine binding pocket allows such an interaction with the WIN motifs of all MLLs.¹³

MLLs have been reported to be essential for embryonic development and biological processes^{14–17} and have been widely implicated in a variety of cancers.^{18–22} As almost all MLLs show minimal or no activity in the absence of the complex components (WDR5 in particular),¹³ identifying WDR5–MLL interaction antagonists has been proposed as a potentially selective alternative to active site directed inhibitors of MLL methyltransferase activity. Such antagonists could serve as a starting point for the development of potential therapeutics to treat MLL-rearranged leukemias or other related cancers.²³

Recent reports detailing the use of short arginine containing peptides to bind WDR5 and disrupt its interaction with MLL,²⁴ along with the use of the WIN motif containing peptides to reduce the levels of H3K4 dimethylation by the MLL core complex *in vitro*,⁹ provide additional rationale for targeting WDR5 as a means to antagonize the MLL and SET1 family of HMTs. However, to the best of our knowledge, the only reported nonpeptide, small molecule antagonist of the WD40-repeat domain is a racemic 1,1'-binaphthyl-2,2'-dicarboxylic acid, SCF-12 (**1**, Figure 1), an inhibitor of yeast Cdc4.²⁵

As part of our ongoing research involving the discovery and development of potent, selective, and cell-permeable small molecule inhibitors (chemical probes) for epigenetic proteins,²⁶

Received: December 20, 2012

Accepted: February 4, 2013

Published: February 4, 2013

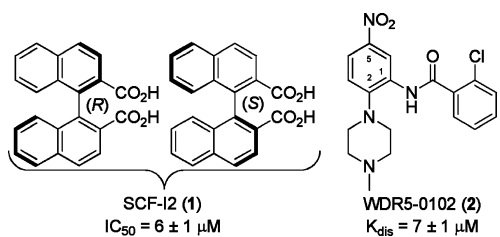


Figure 1. Structures of reported WD40-repeat domain antagonists.

we recently disclosed several novel compounds that antagonize WDR5–MLL interaction, including WDR5-0102 (2) (Figure 1).²³ This proof of principle study prompted us to undertake the SAR-driven optimization of prototypic antagonist WDR5-0102 (2) described in this Letter, leading eventually to preparation of the more potent antagonist 47.

Significantly, a high resolution X-ray crystal structure we obtained for WDR5 in complex with 2 (PDB code 3SMR) showed the compound to be residing within the binding pocket (Figure 2), which normally accommodates the arginine side

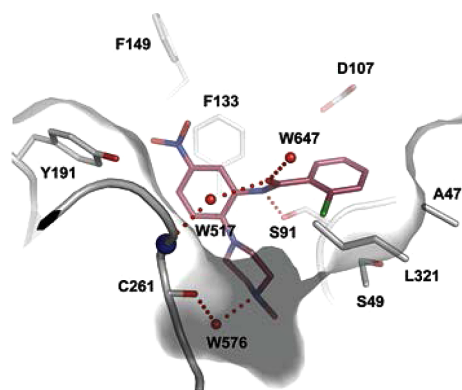
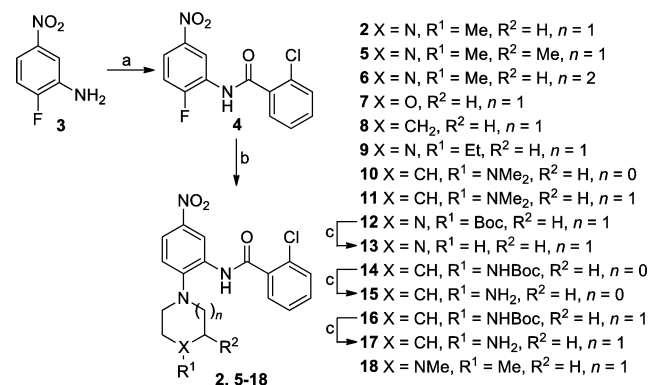


Figure 2. X-ray crystal structure of the WDR5–2 complex (PDB code 3SMR). Compound 2 is in magenta.

chain of H3 peptides and interacting MLL.^{11,12,23} The amide group of 2 forms one direct and one water-mediated (W517) hydrogen bond with the side chain of S91 and the backbone nitrogen of C261, respectively. The *N*-methylpiperazine moiety, predicted to be significantly protonated at physiological pH,²⁷ forms a water-mediated (W576) hydrogen bond with the backbone carbonyl of C261, and it occupies the bottom of the pocket. The 2-chlorophenyl group lies in a shallow, solvent exposed, and largely hydrophobic cavity (also normally occupied by H3 and MLL peptides), surrounded by L321, A47, D107, and the aliphatic portion of the S49 and S91 side chains. Due to the flipping of the F133 and F149 side chains, the nitro group occupies a hydrophobic cleft that is occluded in most WDR5 structures. These distinct structural features suggested a systematic optimization of the core benzamide template through independent variation of the 2-chlorophenyl (benzamide) moiety at position C-1, the *N*-methylpiperazine at C-2, and the nitro substituent at C-5.

An efficient two-step synthetic sequence was developed to first explore the *N*-methylpiperazine region of the scaffold (Scheme 1). Commercially available 2-fluoro-5-nitroaniline (3) was initially reacted with 2-chlorobenzoyl chloride to access 2-chloro-*N*-(2-fluoro-5-nitrophenyl)benzamide (4). Subsequent displacement of the fluorine from this common intermediate using a variety of secondary amines gave rise to the substituted

Scheme 1. Synthesis of Compounds 2 and 4–18^a



^aReagents and conditions: (a) 2-chlorobenzoyl chloride, pyridine, CH₂Cl₂, 4 h, rt. (b) Amine, *N,N*-diisopropylethylamine, DMF, 2 h, 80 °C. (c) Trifluoroacetic acid, CH₂Cl₂, 1 h, rt.

benzamides 2 and 5–18 in high overall yields. In several cases (13, 15, 17), an additional step involving Boc deprotection was required.

These compounds (Table 1) were then evaluated using a fluorescence polarization (FP) assay, detecting the displace-

Table 1. Modifications of the *N*-Methylpiperazine Moiety at C-2

no.	R ¹ (2° amine)	K_{dis} (μM)
2	1-methylpiperazine	6.9 ± 1.5
4	F	>20
5	1,2-dimethylpiperazine	4.7 ± 0.8
6	1-methyl-1,4-diazepane	7.0 ± 1.1
7	morpholine	>20
8	piperidine	>20
9	1-ethylpiperazine	>20
10	<i>N</i> ^{1,1} -dimethylpyrrolidin-3-amine	15.8 ± 2.0
11	<i>N</i> ^{1,1} -dimethylpiperidin-4-amine	>20
13	piperazine	>20
15	pyrrolidin-3-amine	>20
17	piperidin-4-amine	>20
18	<i>N</i> ^{1,1,2} -trimethylethane-1,2-diamine	>20

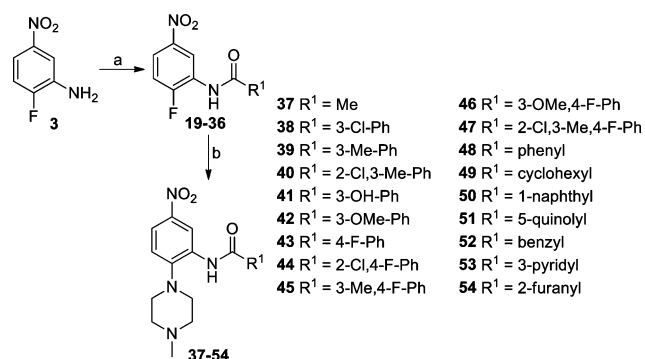
ment of fluorescein-labeled H3(1-15) peptide (ARTKQ-TARKSTGGKA) from its binding pocket in WDR5.²³ In this assay, binding of the fluorescein-labeled peptide to WDR5 ($K_D = 458 \pm 45$ nM) increases the FP signal. Binding compounds compete with and displace the labeled peptide, resulting in the reduction of signal. By monitoring the change in FP signal upon varying the concentration of compounds, $K_{displacement}$ (K_{dis}) values can be calculated by fitting the data to a hyperbolic function as described in the Supporting Information.

We were surprised to see that, despite the available space and potential for hydrogen bond formation with residue D92 at the bottom of the pocket, almost all of the *N*-methylpiperazine modifications produced less active compounds. Demethylation (13), replacement (7–8), and ethylation (9) of the nitrogen proved detrimental, pointing toward the criticality of the water

mediated hydrogen bond to C261, and the effect of conformational and steric constraints within this pocket. Further emphasizing the importance of the *N*-methylpiperazine conformation is ring-opened compound **18**, which also showed a dramatic loss in activity. Only slight expansion of the ring (**6**) produced a viable compound equipotent to **2**, while ring contraction (**10**) resulted in a 2-fold loss of potency. While efforts at forming hydrogen bonds at the bottom of the pocket with compounds **11** and **17** failed, methylated compound **5** was tolerated. However, given the cost and availability of 1,2-dimethylpiperazine, we opted to retain the original *N*-methylpiperazine moiety for the synthesis of subsequent analogs.

To vary the benzamide moiety, a modified two-step synthetic sequence was employed (Scheme 2). Commercially available 2-

Scheme 2. Synthesis of Compounds 37–54^a



^aReagents and conditions: (a) R¹COCl, pyridine, CH₂Cl₂, 4 h, rt. (b) 1-Methylpiperazine, *N,N*-diisopropylethylamine, DMF, 2 h, 80 °C.

fluoro-5-nitroaniline (**3**) was used once again, but now it reacted with a series of different acid chlorides to afford substituted *N*-(2-fluoro-5-nitrophenyl)benzamides **19–36**. Displacement of the fluorine with *N*-methylpiperazine proceeded as before, giving rise to the substituted benzamides **37–54** in high overall yields.

In general, modifications of the benzamide moiety proved to have a more variable impact on potency (Table 2). The fundamental need for an aromatic substituent directly attached to the carbonyl of the benzamide is made clear by the relative activity of compounds **37**, **49**, and **52** versus compound **48**. Reducing the size of this aromatic substituent (**54**) appears detrimental, while increasing its size (**50**) affords a substantial gain in potency, resulting from greater surface interactions with the hydrophobic pocket.

Interestingly, the introduction of a nitrogen into the aromatic moiety (**51** and **53**) reduces activity (versus parent compounds **50** and **48**, respectively), failing to make any hydrogen bond interactions. Particularly significant are variable substitutions made at the 3-position of the aromatic ring (**38–42**), all of which, with the exception of **41**, resulted in an appreciable potency gain. Interestingly, further gains in potency were achievable through monofluorination at the 4-position of **2**, **40**, **39**, **42**, and **48**, leading to 10-fold (**44**), 4-fold (**47**), and 2-fold (**45–46**, **43**) more active compounds, respectively. While the 4-F substituent may serve to increase potencies by strengthening the amide-to-S91 hydrogen bond interaction via an electron withdrawing effect, such a rationale requires further investigation. It should be noted that, with a 25-fold greater potency

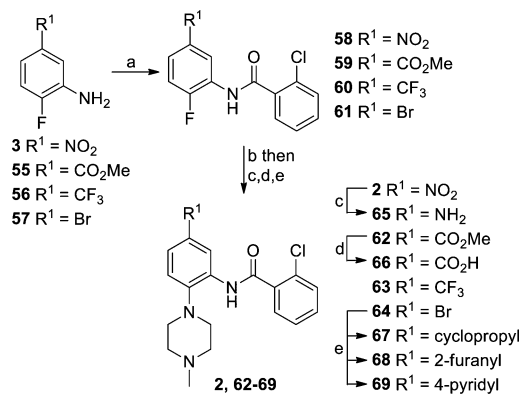
Table 2. Modifications of the 2-Chlorophenyl (Benzamide) Moiety at C-1

no.	R ¹	K _{dis} (μM)
2	2-Cl-phenyl	6.9 ± 1.5
37	Me	>10
38	3-Cl-phenyl	1.8 ± 0.1
39	3-Me-phenyl	1.1 ± 0.1
40	2-Cl-3-Me-phenyl	1.1 ± 0.1
41	3-OH-phenyl	>10
42	3-OMe-phenyl	1.4 ± 0.1
43	4-F-phenyl	3.1 ± 0.3
44	2-Cl-4-F-phenyl	0.63 ± 0.1
45	3-Me-4-F-phenyl	0.59 ± 0.1
46	3-OMe-4-F-phenyl	0.68 ± 0.1
47	2-Cl-3-Me-4-F-phenyl	0.27 ± 0.1
48	phenyl	5.8 ± 0.4
49	cyclohexyl	>10
50	1-naphthyl	0.71 ± 0.1
51	5-quinolyl	1.5 ± 0.2
52	benzyl	>10
53	3-pyridyl	>10
54	2-furanyl	>10

versus the series parent **2**, **47** is the most significant compound synthesized in this study.

The same core, two-step sequence used to prepare the benzamide analogs **37–54** was used once again to introduce substituents modifying the prototypic nitro group at C-5 to give compounds **62–69** (Scheme 3). In this instance, however, the sequence was also initiated with a number of 2-fluoroanilines (**55–57**) variably substituted at the 5-position, allowing for access to final compounds **62–64** and **66–69**. Reduction and hydrolysis were used to generate compounds **65** and **66** from **2**

Scheme 3. Synthesis of Compounds 2 and 62–69^a

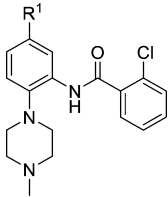


^aReagents and conditions: (a) 2-chlorobenzoyl chloride, pyridine, CH₂Cl₂, 4 h, rt. (b) 1-Methylpiperazine, *N,N*-diisopropylethylamine, DMF, 2 h, 80 °C. (c) SnCl₂, conc HCl, 1 h, 60 °C. (d) LiOH·H₂O, THF/H₂O, 1 h, rt. (e) R¹B(OH)₂, Pd(PPh₃)₄ (cat.), Na₂CO₃, toluene/H₂O (1:1), 16 h, 110 °C.

and **62** respectively, while compounds **67–69** were accessible via Suzuki coupling from precursor **64**.

Variations of the C-5 position substituent proved disappointing, producing largely inactive compounds (Table 3). Protic

Table 3. Modifications of the Nitro Group at C-5



no.	R ¹	K _{dis} (μM)
2	NO ₂	6.9 ± 1.5
62	CO ₂ Me	6.6 ± 1.1
63	CF ₃	>10
64	Br	>10
65	NH ₂	>10
66	CO ₂ H	>10
67	cyclopropyl	>10
68	2-furanyl	3.5 ± 0.3
69	4-pyridyl	2.2 ± 0.1

groups such as amine (**65**) and acid (**66**) were not tolerated within the hydrophobic cleft, although the ester (**62**) was accepted. While this was known from our previous work,²³ we opted to conduct the optimization outlined in this letter using the nitro group at C-5, both for ease of synthesis and to limit any potential liability arising from ester hydrolysis in eventual cell-based studies. While smaller substituents (**63–64**, **67**) also failed to produce active compounds, the introduction of larger aromatic groups such as 2-furan (**68**) or 4-pyridine (**69**) did allow for a modest 2- or 3-fold potency increase. This observation also opens the possibility of further enlarging the C-5 position substituent to more fully occupy the hydrophobic cleft, and potentially engage Y191.

We had previously shown that positioning of the benzamide ring in the shallow side cavity of the binding site can be shifted depending on the type and position of its substituents, with potentially significant impact on activity.²³ To better understand the increased potency of compound **47**, we solved its structure in complex with WDR5 (PDB code 4IA9) (Figure 3). As expected, the compound occupies the central cavity of WDR5 and recapitulates interactions previously observed with less potent analogs (PDB codes 3SMR and 3UR4), including direct and water mediated hydrogen bonds with S91 and C261, opening-up of a cavity occupied by the nitro group, and aromatic stacking with F133.²³ The conformation of side chains within 4 Å of the compound is almost perfectly conserved (RMSD = 0.15 Å). The scaffold sits in the pocket, adopting a conformation closer to that observed for the 2-chlorophenyl analog (RMSD = 0.33 Å, PDB code 3SMR) versus that of the 3-methoxyphenyl analog (RMSD = 1.47 Å, PDB code 3UR4). The new structure clearly shows that the 3-methyl and 4-fluoro substituents bring hydrophobic interactions with side-chains lining the binding pocket and that the section of the ring facing D107 remains unsubstituted, suggesting avenues for further optimization.

Overall, by independently modifying the benzamide, C-2, and C-5 position substituents on parent compound **2**, we were ultimately able to realize a greater than 25-fold gain in potency

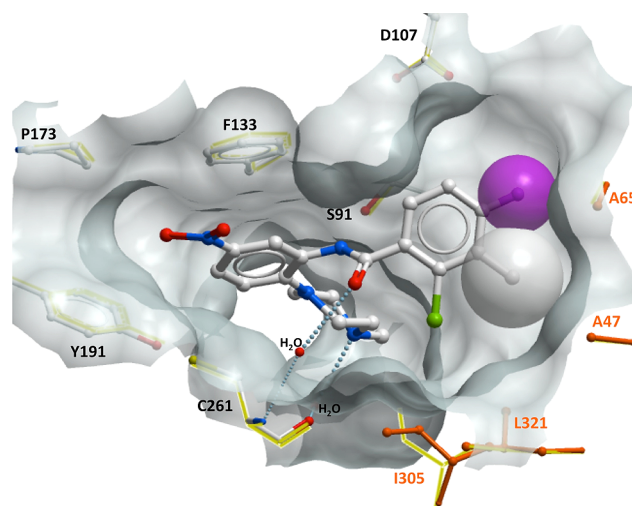


Figure 3. X-ray crystal structure of the WDR5–47 complex (PDB code 4IA9). Compound **47** (gray sticks) binds in the central cavity of WDR5. Addition of methyl and fluoro substituents at positions 3 and 4 of the 2-chlorophenyl moiety optimizes occupancy of the side cavity and introduces additional interactions with surrounding hydrophobic side chains (orange). Color coding: white, carbon; red, oxygen; blue, nitrogen; green, chlorine; magenta, fluorine.

through the synthesis of compound **47**. Having begun to establish the parameters of moieties tolerated within the WDR5 binding site regions, we intend to leverage this information for the continued structure-based design and development of new compounds for antagonism of the WDR5–MLL interaction.

■ ASSOCIATED CONTENT

📄 Supporting Information

Synthetic experimental procedures, analytical and spectral characterization data of all synthesized compounds, and details of biochemical assay methods. This material is available free of charge via the Internet at <http://pubs.acs.org>.

■ AUTHOR INFORMATION

✉ Corresponding Author

*D.S.: tel, +1 (416) 946-0132; fax, +1 (416) 946-0880; e-mail, david.smil@utoronto.ca. M.V.: tel, +1 (416) 432-1980; fax, +1 (416) 946-0588; e-mail, m.vedadi@utoronto.ca.

👤 Author Contributions

[§]These authors contributed equally to this work. Y.B. and M.G. designed and synthesized compounds, and contributed to editing of the paper. E.K. and G.A.W. performed all FP assays (Table 1, 2 and 3). T.H. purified protein for assays. G.P. and K.T.N. contributed to the design of compounds. H.W. and L.D. purified and co-crystallized WDR5 with compound **47**. A.D. determined the crystal structure of WDR5–47. G.S. performed binding assays (Supplementary Figure 1). M.S. contributed to the design of compounds, analyzed the WDR5–47 co-structure (Figure 2 and Figure 3), and wrote the paper. C.H.A., P.J.B. and R.A. contributed to experimental design and editing of the paper. M.V. and D.S. reviewed data, contributed to overall experimental design, and wrote the paper. M.V. was the principal investigator, designed experiments, analysed data and supervised the assay and compound evaluation process. D.S. designed and synthesized compounds, and supervised all chemistry efforts.

Funding

The Structural Genomics Consortium is a registered charity (number 1097737) that receives funds from the Canadian Institutes for Health Research, Genome Canada, the Canadian Foundation for Innovation, the Ontario Innovation Trust, the Ontario Ministry for Research and Innovation, the Wellcome Trust, AbbVie, Eli Lilly Canada, GlaxoSmithKline, Novartis, Pfizer, and Takeda. Ontario Institute for Cancer Research funding is provided by the Government of Ontario through the Ontario Ministry of Economic Development and Innovation.

Notes

The authors declare no competing financial interest.

ACKNOWLEDGMENTS

We would like to thank Dr. Ahmed Aman and Dr. Taira Kiyota for assistance in obtaining the high resolution mass spectra (HRMS) of all final synthesized compounds.

REFERENCES

- (1) Shilatifard, A. Molecular implementation and physiological roles for histone H3 lysine 4 (H3K4) methylation. *Curr. Opin. Cell Biol.* **2008**, *20*, 341–348.
- (2) Ruthenburg, A. J.; Allis, C. D.; Wysocka, J. Methylation of lysine 4 on histone 3: intricacy of writing and reading a single epigenetic mark. *Mol. Cell* **2007**, *25*, 15–30.
- (3) Kouzarides, T. Chromatin modifications and their function. *Cell* **2007**, *128*, 693–705.
- (4) Ernst, P.; Vakoc, C. R. WRAD: enabler of the SET1-family of H3K4 methyltransferases. *Briefings Functional Genomics* **2012**, *11*, 217–226.
- (5) Dou, Y.; Milne, T. A.; Ruthenburg, A. J.; Lee, S.; Lee, J. W.; Verdine, G. L.; Allis, C. D.; Roeder, R. G. Regulation of MLL1 H3K4 methyltransferase activity by its core components. *Nat. Struct. Mol. Biol.* **2006**, *13*, 713–719.
- (6) Wysocka, J.; Swigut, T.; Milne, T. A.; Dou, Y.; Zhang, X.; Burlingame, A. L.; Roeder, R. G.; Brivanlou, A. H.; Allis, C. D. WDR5 associates with histone H3 methylated at K4 and is essential for H3 K4 methylation and vertebrate development. *Cell* **2005**, *121*, 859–872.
- (7) Steward, M. M.; Lee, J.-S.; O'Donovan, A.; Wyatt, M.; Bernstein, B. E.; Shilatifard, A. Molecular regulation of H3K4 trimethylation by ASH2L, a shared subunit of MLL complexes. *Nat. Struct. Mol. Biol.* **2006**, *13*, 852–854.
- (8) Patel, A.; Dharmarajan, V.; Cosgrove, M. S. Structure of WDR5 bound to mixed lineage leukemia protein-1 peptide. *J. Biol. Chem.* **2008**, *283*, 32158–32161.
- (9) Patel, A.; Vought, V. E.; Dharmarajan, V.; Cosgrove, M. S. A conserved arginine-containing motif crucial for the assembly and enzymatic activity of the mixed lineage leukemia protein-1 core complex. *J. Biol. Chem.* **2008**, *283*, 32162–32175.
- (10) Schuetz, A.; Allali-Hassani, A.; Martin, F.; Loppnau, P.; Vedadi, M.; Bochkarev, A.; Plotnikov, A. N.; Arrowsmith, C. H.; Min, J. Structural basis for molecular recognition and presentation of histone H3 by WDR5. *EMBO J.* **2006**, *25*, 4245–4252.
- (11) Avdic, V.; Zhang, P.; Lanouette, S.; Groulx, A.; Tremblay, V.; Brunzette, J.; Couture, J.-F. Structural and biochemical insights into MLL1 core complex assembly. *Structure* **2011**, *19*, 101–108.
- (12) Ruthenburg, A. J.; Wang, W.; Graybosch, D. M.; Li, H.; Allis, C. D.; Patel, D. J.; Verdine, G. L. Histone H3 recognition and presentation by the WDR5 module of the MLL1 complex. *Nat. Struct. Mol. Biol.* **2006**, *13*, 704–712.
- (13) Zhang, P.; Lee, H.; Brunzelle, J. S.; Couture, J.-F. The plasticity of WDR5 peptide-binding cleft enables the binding of the SET1 family of histone methyltransferases. *Nucleic Acids Res.* **2012**, *40*, 4237–4246.
- (14) Terranova, R.; Agherbi, H.; Boned, A.; Meresse, S.; Djabali, M. Histone and DNA methylation defects at Hox genes in mice expressing a SET domain-truncated for of Mll1. *Proc. Natl. Acad. Sci. U.S.A.* **2006**, *103*, 6629–6634.
- (15) Argiropoulos, B.; Humphries, R. K. Hox genes in hematopoiesis and leukemogenesis. *Oncogene* **2007**, *26*, 6766–6776.
- (16) Rampalli, S.; Li, L.; Mak, E.; Ge, K.; Brand, M.; Tapscott, S. J.; Dilworth, F. J. p39 MAPK signaling regulates recruitment of Ash2L-containing methyltransferase complexes to specific genes during differentiation. *Nat. Struct. Mol. Biol.* **2007**, *14*, 1150–1156.
- (17) Lim, D. A.; Huang, Y.-C.; Swigut, T.; Mirick, A. L.; Garcia-Verdugo, J. M.; Wysocka, J.; Ernst, P.; Alvarez-Buylla, A. Chromatin remodeling factor MLL1 is essential for neurogenesis from postnatal neural stem cells. *Nature* **2009**, *458*, 529–533.
- (18) Ruault, M.; Brun, M. E.; Ventura, M.; Roizès, G.; De Sario, A. MLL3, a new human member of the TRX/MLL gene family, maps to 7q36, a chromosome region frequently deleted in myeloid leukaemia. *Gene* **2002**, *284*, 73–81.
- (19) Liedtke, M.; Cleary, M. L. Therapeutic targeting of MLL. *Blood* **2009**, *113*, 6061–6068.
- (20) Tkachuk, D. C.; Kohler, S.; Cleary, M. L. Involvement of a homolog of Drosophila trithorax by 11q23 chromosomal translocations in acute leukemias. *Cell* **1992**, *71*, 691–700.
- (21) Gu, Y.; Nakamura, T.; Alder, H.; Prasad, R.; Canaani, O.; Cimino, G.; Croce, C. M.; Canaani, E. The t(4;11) chromosome translocation of human acute leukemias fuses the ALL-1 gene, related to Drosophila trithorax, to the AF-4 gene. *Cell* **1992**, *71*, 701–708.
- (22) Krivtsov, A. V.; Armstrong, S. A. MLL translocations, histone modifications and leukemia stem-cell development. *Nat. Rev. Cancer* **2007**, *7*, 823–833.
- (23) Senisterra, G.; Wu, H.; Allali-Hassani, A.; Wasney, G. A.; Barsyte-Lovejoy, D.; Dombrowski, L.; Dong, A.; Nguyen, K. T.; Smil, D.; Bolshan, Y.; Hajian, T.; He, H.; Seitova, A.; Chau, I.; Li, F.; Poda, G.; Couture, J.-F.; Brown, P. J.; Al-awar, R.; Schapira, M.; Arrowsmith, C. H.; Vedadi, M. Small molecule inhibition of MLL activity by disruption of its interaction with WDR5. *Biochem. J.* **2013**, *449*, 151–159.
- (24) Karatas, H.; Townsend, E. C.; Cao, F.; Chen, Y.; Bernard, D.; Liu, L.; Lei, M.; Dou, Y.; Wang, S. High-affinity, small-molecule peptidomimetic inhibitors of MLL1/WDR5 protein-protein interaction. *J. Am. Chem. Soc.* **2013**, *135*, 669–682.
- (25) Orlicky, S.; Tang, X.; Neduva, V.; Elowe, N.; Brown, E. D.; Sicheri, F.; Tyers, M. An allosteric inhibitor of substrate recognition by the SCF^{Cdc4} ubiquitin ligase. *Nat. Biotechnol.* **2010**, *28*, 733–737.
- (26) Edwards, A. M.; Bountra, C.; Kerr, D. J.; Willson, T. M. Open access chemical and clinical probes to support drug discovery. *Nat. Chem. Biol.* **2009**, *5*, 436–440.
- (27) Protonation states of the compounds were predicted using ChemAxon's pK_a-calculator (www.chemaxon.com).